JOURNAL OF AGRICULTURAL AND FOOD CHEMISTRY

Article

pubs.acs.org/JAFC

Identification of Three Novel Polyphenolic Compounds, Origanine A−C, with Unique Skeleton from *Origanum vulgare* L. Using the Hyphenated LC-DAD-SPE-NMR/MS Methods

Hongbing Liu,[†,‡,§] Anmin Zheng,[†,§] Huili Liu,[†] Haiyan Yu,[†] Xiangyu Wu,[†,‡] Chaoni Xiao,[†,∥] Hui Dai,[†,⊥] Fuhua Hao,[†] Limin Zhang,[†] Yulan Wang,[†] and Huiru Tang[†,*]

[†]State Key Laboratory of Magnetic Resonance and Atomic and Molecular Physics, Wuhan Centre for Magnetic Resonance, Wuhan Institute of Physics and Mathematics, Chinese Academy of Sciences, Wuhan 430071, P. R. China

[∥]College of Life Sciences, Northwest University, Xi'an 710069, P. R. China

[⊥]Department of Physiology and Pathophysiology, Peking University, Beijing 100191, P. R. China

[‡]Graduate School of the Chinese Academy of Sciences, Beijing 100049, P. R. China

Supporting Information

ABSTRACT: Identification of new compounds especially those with new skeletons from plant kingdom has long been a vital aspect for understanding phytochemistry, plant metabolisms and discovering new bioactive compounds. In this study, we identified and isolated three novel polyphenolic compounds, origanine A−C, from a well-researched plant *Origanum vulgare* L. using the hyphenated LC-DAD-SPE-NMR/MS methods. Based on the combined information from UV−visible, accurate mass and 2D NMR spectra together with computational calculations, we found that these compounds all had a novel skeleton of cyclohexenetetracarboxylic acids attached with some well-known bioactive moieties including 3,4-dihydroxyphenyl, 4-(β-D-glucopyranosyloxy)benzyl alcohol (gastrodin), and 3-(3,4-dihydroxyphenyl)lactic acid (danshensu) residues. These findings provided crucial information to fill the gaps in our knowledge in terms of the plant secondary metabolism. This study also indicated the necessity for further research in plant secondary metabolism for even well-studied plants and demonstrated the powerfulness of the hyphenated LC-DAD-SPE-NMR/MS methods for comprehensive analysis of plant metabolites in particular for discovering new natural compounds.

KEYWORDS: *Origanum vulgare L., polyphenolic compounds, cyclohexenetetracarboxylic acids, LC-DAD-SPE-NMR/MS, origanine A−C, computational calculations*

INTRODUCTION

Plants in the Lamiaceae family are well-known for their richness in secondary metabolites such as polyphenolic compounds[1−4] which have potent *in situ* antioxidative activities,[5,6] and essential oils with various biological activities.[7] The genus *Origanum* in this family has more than 40 species,[1] and most of them are indigenous to the Mediterranean regions. Among all these species, *O. vulgare* L. is by far the most widespread species with its presence in Europe, north Africa, America and Asia, where this plant has been used as a culinary herb and a traditional medicine for a long time.[1]

The secondary metabolites of this plant have been well studied in terms of polyphenolic compounds and essential oils. Consequently, more than one hundred nonvolatile compounds have already been identified in this plant with conventional phytochemistry methods including flavonoids, depsides and origanosides.[7−13] However, such methods often stress the abundant and easy-to-separate compounds with a number of compounds easily missed. Therefore, it remains unclear whether some novel compounds with new skeletons are still to be discovered even though identification of such novel metabolites is crucially important for drug discoveries and understanding plant metabolism. Such curiousity becomes even more encouraged with recent identification of a number of novel compounds in the well-studied *Rosmarinus officinalis* L.[14] and *Salvia miltiorrhiza* Bunge[15,16] in this family. This was only made possible with the hyphenated LC-DAD-SPE-NMR/MS methods[14−18] enabling comprehensive analysis of the complex plant metabolite mixtures including both the primary and secondary metabolites. In fact, recent development of the combined NMR and LC-DAD-MS methods has made it possible to achieve the metabonome-wide analysis of plant metabolites.[14−16,19−23] This is because the combined approaches facilitate the combined advantages of these techniques, enabling efficient composition ananlysis of the plant metabolites in the complex mixtures including both primary and secondary metabolites.

In this work, we report the discovery of three new polyphenolic acids from *O. vulgare* L. using the hyphenated LC-DAD-SPE-NMR/MS methods. Complete elucidation of their structures revealed that all these compounds had a novel skeleton of cyclohexenetetracarboxylic acids attached with some well-known polyphenolic moieties including 3,4-dihydroxyphenyl, 4-(β-D-glucopyranosyloxy)benzyl alcohol

Received: October 28, 2011
Revised: December 3, 2011
Accepted: December 5, 2011
Published: December 5, 2011

(gastrodin) and 3-(3,4-dihydroxyphenyl)lactic acid (danshensu) moieties.

MATERIALS AND METHODS

Chemicals. HPLC grade acetonitrile was purchased from J. T. Baker Pharmaceuticals Company (Phillipsburg, NJ), and analytical grade formic acid was purchased from Sinopharm Chemical Reagent Co. Ltd. (Shanghai, China). Deuterated acetonitrile-d_3 (99.8%) was obtained from Cambridge Isotopes Laboratories (Andover, MA). Ultrapure water was produced in Milli-Q Water Purification System (Milfold, MA).

Plant Materials and Sample Preparation. The samples of *O. vulgare* L. were collected in 2007 in the mountainous regions of Tuanfeng County (Hubei, China). Positive species identification of this plant was made by Prof. Jianqiang Li of Wuhan Botanical Garden, Chinese Academy of Sciences; a voucher specimen was deposited at the herbarium of Wuhan Botanical Garden (sample code: Liuhongbing001). The air-dried and powdered leaves (0.2 g) were extracted ultrasonically with aqueous acetonitrile (50%, 2 mL) twice. The combined supernatants were lyophilized after removal of organic solvent under vacuum. The dried materials were then sealed in eppendorf tubes and stored in dry and dark conditions until further analysis.

LC-DAD-ESI-Q-TOF-MS Analysis. The dry extract (20 mg) was dissolved in 1 mL of 50% aqueous acetonitrile followed with filtration through a 0.4 μm filter. The chromatographic separation was performed on an Agilent 1200 HPLC system equipped with an online degasser, a quaternary solvent delivery system, an autosampler, a diode-array detector (DAD) and a **micrOTOF**-Q mass spectrometer (Bruker Daltonics, Germany) with an Apollo electrospray ionization (ESI) source. An analytical ACE column (C18, 250 × 4.6 mm, 5 μm) was used with a flow rate of 1.0 mL/min and the column oven temperature of 35 °C. The mobile phase consisted of A (0.1% formic acid in H_2O) and B (acetonitrile) with the solvent gradient varying from 5% B to 15% B in the first 15 min and then to 25% B up to 45 min. A 5 μL sample was injected to the LC system, and the chromatogram was monitored at 280 nm. A T-piece was used as a splitter so that analytes from the ACE column were detected by the DAD detector and MS system in parallel with only about 5% eluent directed to the mass spectrometer. The acquisition of high resolution mass spectra was conducted in the negative ion mode with a nebulizer nitrogen gas pressure of 0.8 bar, dry gas flow rate of 8.0 L/min and gas temperature of 200 °C. Capillary voltage was set to +4000 V, and the end plate offset was set to 500 V. The MS data was recorded with a range of m/z 50−2000.

For LC-DAD-SPE-NMR studies, the chromatographic separation of the extract of *O. vulgare* L. was performed on the same system with the same elution parameters. In this case, a 20 μL sample was injected for each run to trap more analytes without compromising the chromatographic separation. A Spark-Holland SPE system was hyphenated to HPLC; the 280 nm UV absorption was used to monitor the chromatographic separation and to set the absorbance threshold for triggering the SPE trapping. In order to lower the eluotropic strength, a dilution flow of water was added to the eluent at 3.0 mL/min with a K-120 makeup pump (Knauer, Berlin, Germany) prior to SPE trapping. The Hysphere GP (10 × 2 mm) SPE cartridges (Spark, Holland) were conditioned with 500 μL of acetonitrile before use followed by equilibration with 500 μL of water. In order to trap enough materials for structrure elucidation with 1D and 2D NMR spectroscopy, ten repeated LC runs were performed and three concerned peaks were trapped on three different SPE cartridges, respectively. The SPE cartridges were then dried with a flow of nitrogen gas for 30 min. The trapped compounds were then eluted with 200 μL of CD_3CN into an NMR detection flowcell (60 μL) inserted in a CryoProbe via a fused-silica capillary for NMR experiments. These three compounds were then collected and redisolved into 2.5 mm NMR capillary tubes (CD_3CN), respectively, for further NMR analysis once required.

NMR Experiments. All NMR data were acquired on a Bruker Avance III 800 MHz spectrometer equipped with a 5 mm cryogenic TCI probe and 60 μL Cryofit (Bruker, Rheinstetten, Germany). Hystar (V.2.0) and Topspin (V.2.1) software packages (Bruker, Rheinstetten, Germany) were used for LC-DAD-SPE-NMR data acquisition and processing. ^{1}H NMR spectra were recorded with 16−32 scans, 32k data points, spectra width of 20 ppm, and recycle delay of 3.6 s. 2D NMR spectra were recorded and processed in a similar fashion as reported previously[14−16] with slightly different parameters. To be specific, ^{1}H−^{1}H COSY, TOCSY and ^{1}H−^{13}C HSQC 2D NMR spectra were acquired with 2048 data points and 4 scans for each of 256 increments. ^{1}H−^{13}C HMBC 2D NMR spectra were acquired with 2048 data points and 16−48 scans for each of 256 or 512 increments. For both HSQC and HMBC experiments, $^1J_{C-H}$ was set to 145 Hz and $^nJ_{C-H}$ was set to 6 Hz. Spectral widths were adjusted to cover all signals for each individual sample but to maximize digital resolutions. ^{1}H and ^{13}C chemical shifts were referenced to solvent signals of CD_3CN (δ_H = 1.94 and δ_C = 118.7). For 2D NMR spectra, the data were zero-filled to 2 × 2 k matrices prior to Fourier Transformation with appropriate window functions and forward linear predictions.

RESULTS AND DISCUSSION

In the LC-DAD-ESI-Q-TOF-MS chromatogram (Figure 1) of the leaf extracts of *O. vulgare* L., several peaks (peaks 4−7 in

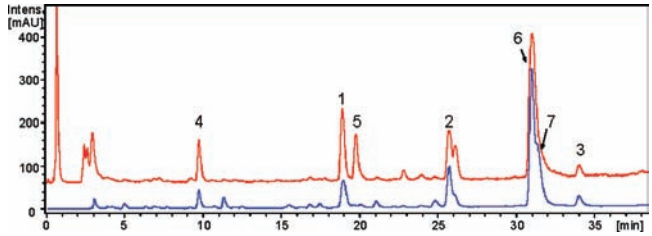

Figure 1. LC-DAD-ESI-Q-TOF-MS chromatogram of the raw extract of *Origanum vulgare* L. leaves. Blue trace: UV 280 nm chromatogram. Red trace: total ion chromatogram (TIC). Peak 4: danshensu (MS with −ve: m/z 197.0470). Peak 5: 12-hydroxyjasmonic acid 12-O-β-D-glucopyranoside (MS with −ve: m/z 387.1664). Peak 6: 4-(3,4-dihydroxybenzoyloxymethyl)phenyl-*O*-β-D-glucopyranoside (MS with −ve: m/z 421.1138). Peak 7: luteolin 7-*O*-β-D-glucuronide (MS with −ve: m/z 461.0470). Peaks 1−3: three novel compounds (see Figure 2 for their MS data).

Figure 1) are readily identified as danshensu, 12-hydroxyjasmonic acid 12-*O*-β-D-glucopyranoside,[8] 4-*O*-β-D-glucopyranosylbenzyl-3′,4′-dihydroxylbenzoate[12] and luteolin 7-*O*-β-D-glucuronide,[10] respectively, based on literature data. However, three chromatographic peaks (peaks 1−3 in Figure 1) were judged to be new compounds in this species or completely novel compounds with their mass spectra (in the negative ion mode) showing *quasimolecular* ions at m/z 633.1470, 813.1896 and 813.1864, respectively (Figure 2). The loss of 44 Da in their MS spectra (Figure 2) and UV absorbances (λ_{max}: 282−286, 310−335 nm, Figure S1 in the Supporting Information) suggested the presence of −COOH groups and aromatic rings in their structures. Their LC peaks were then repeatedly trapped on three different microcartridges, respectively, followed with thorough NMR analysis (Figure S2−S18 in the Supporting Information) to obtain their structures (Figure 3). Since they were all from *Origanum vulgare* L., we named them as origanine A−C.

Origanine A (**1**) showed a *quasimolecular* ion at m/z 633.1470 in the negative ion mode (Figure 2A), and thus $C_{29}H_{30}O_{16}$ was suggested to be its molecular formula (calcd m/z 633.1461 for $C_{29}H_{29}O_{16}$, with an error of 0.9 mDa). The number of carbons was further confirmed with ^{1}H−^{13}C HMBC 2D NMR (Figure S7 in the Supporting Information).

dx.doi.org/10.1021/jf204406u | J. Agric.Food Chem. 2012, 60, 129−135

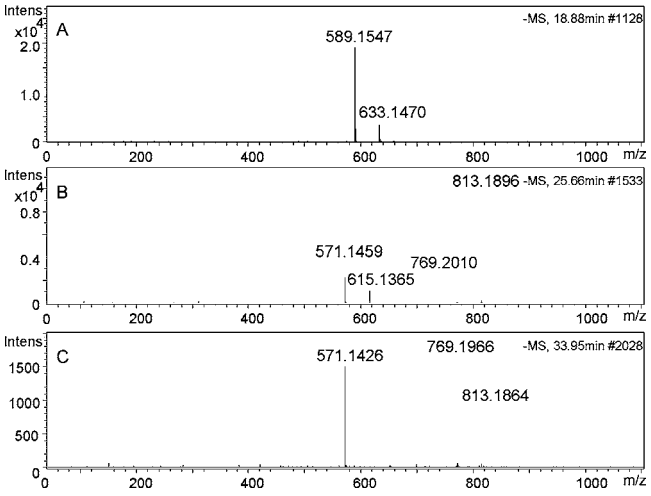

Figure 2. MS spectra of three novel compounds detected from the extract of *Origanum vulgare* L. leaves in the LC-DAD-ESI-Q-TOF-MS analysis. (A) Origanine A ($C_{29}H_{30}O_{16}$, calcd m/z 633.1461). (B) Origanine B ($C_{38}H_{38}O_{20}$, calcd m/z 813.1884). (C) Origanine C ($C_{38}H_{38}O_{20}$, calcd m/z 813.1884).

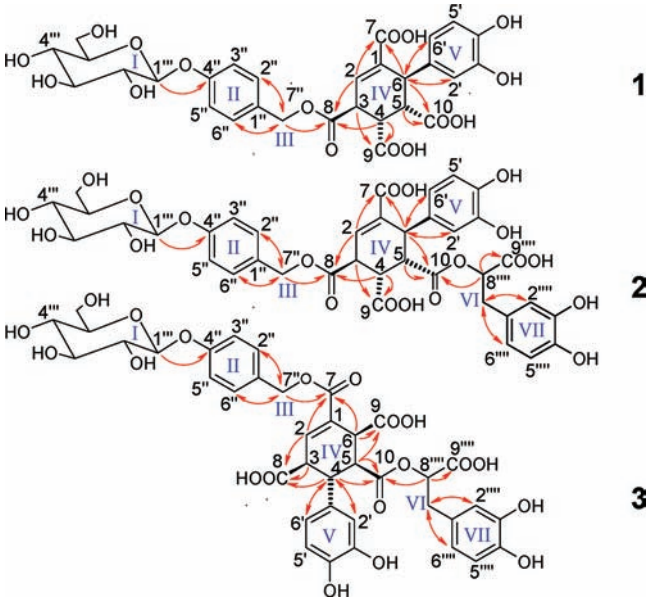

Figure 3. Structural features for origanine A (**1**), B (**2**) and C (**3**). I–VII: key structural fragments. Red arrows: key long-range correlations observed in $^1H-^{13}C$ HMBC 2D NMR spectra.

The atomic connectivities (or planar structure) of **1** was established with a catalogue of 2D NMR spectra (Figures S3–S7 in the Supporting Information). Five different $^1H-^1H$ coupling systems in the $^1H-^1H$ TOCSY spectrum (Figure S4 in the Supporting Information) suggested the presence of five structural fragments (I–V) including three aliphatic and two aromatic ones (Figure 3). Fragment I showed a typical signal pattern for a β-glucoside moiety with seven protons at δ_H 4.94 (1H, d, J = 7.5 Hz, H1‴), 3.39 (1H, dd, J = 9.0, 7.5 Hz, H2‴), 3.40 (1H, dd, J = 9.0, 8.4 Hz, H3‴), 3.32 (1H, dd, J = 9.6, 8.4 Hz, H4‴), 3.46 (1H, ddd, J = 9.6, 6.0, 2.6 Hz, H5‴), 3.82 (1H, dd, J = 12.0, 2.6 Hz, H6‴a) and 3.62 (1H, dd, J = 12.0, 6.0 Hz, H6‴b), which was confirmed with data from $^1H-^1H$ COSY (Figure S3 in the Supporting Information), $^1H-^{13}C$ HSQC (Figure S6 in the Supporting Information) and HMBC 2D NMR spectra (Figure S7 in the Supporting Information). Fragment II had a para-substituted phenyl structure showing a typical AA′BB′ coupling system with proton signals at δ_H 7.36 (2H, d, J = 8.7 Hz, H2″, 6″) and 7.07 (2H, d, J = 8.7 Hz, H3″, 5″). $^1H-^{13}C$ HSQC and HMBC spectra of this compound (Figures S6 and S7 in the Supporting Information) confirmed one substitution as an oxygen-based group. Fragment III was a $-CH_2O-$ moiety with two geminal protons at δ_H 5.20 (1H, d, J = 12.1 Hz, H7″a) and 5.12 (1H, d, J = 12.1 Hz, H7″b). Fragment IV has a five substituted cyclohexene struture with five correlated protons in its TOCSY spectrum (Figure S4 in the Supporting Information) at δ_H 7.01 (1H, d, J = 3.3 Hz, H2), 3.88 (1H, ddd, J = 10.3, 3.3, 1.8 Hz, H3), 3.03 (1H, dd, J = 10.3, 3.9 Hz, H4), 3.26 (1H, dd, J = 3.9, 2.2 Hz, H5) and 4.32 (1H, br dd, J = 2.2, 1.8 Hz, H6). Sequential positions of these protons were determined as δ_H 7.01–3.88–3.03–3.26–4.32 with $^1H-^1H$ COSY 2D NMR spectrum (Figure S3 in the Supporting Information); the correlation observed for δ_H 3.88–4.32 was also normal for this type of structure.[24] Fragment V was a 3,4-dihydroxyphenyl group with a typical ABX coupling system for protons at δ_H 6.41 (1H, dd, J = 8.2, 2.2 Hz, H6′), 6.69 (1H, d, J = 8.2 Hz, H5′) and 6.66 (1H, d, J = 2.2 Hz, H2′) in both $^1H-^1H$ COSY (Figure S3 in the Supporting Information) and TOCSY (Figure S4 in the Supporting Information) 2D NMR spectra. This was further confirmed with the $^1H-^{13}C$ HSQC (Figure S6 in the Supporting Information) and HMBC (Figure S7 in the Supporting Information) data.

Furthermore, linkages between these fragments were established using heteronuclear 2D NMR spectra (Figures S6 and S7 in the Supporting Information) with the direct H–C correlations determined based on $^1H-^{13}C$ HSQC data (Table 1, Figure S6 in the Supporting Information). Its $^1H-^{13}C$ HMBC 2D NMR spectrum (Figure S7 in the Supporting Information) showed that fragment I (β-glucosyl moiety) and fragment III ($-CH_2O-$) were two substitutents for fragment II with long-range correlations (Figure S7 in the Supporting Information) for H1‴/C4″ (δ_H 4.94/δ_C 158.9), H7″a/C1″ (δ_H 5.20/δ_C 131.3) and H7″b/C1″ (δ_H 5.12/δ_C 131.3). This was further supported by correlations for H7″a/C2″ (δ_H 5.20/δ_C 131.2), H7″b/C2″ (δ_H 5.12/δ_C 131.2) and H2″/C7″(δ_H 7.36/δ_C 68.1) in its $^1H-^{13}C$ HMBC 2D NMR spectrum (Figure S7 in the Supporting Information). Therefore, fragments I–III were linked together in the form of a 4-(β-D-glucopyranosyloxy)benzyl alcohol (gastrodin) moiety. Correlations between both protons of $-CH_2O-$ (δ_H 5.20, 5.12) and a carboxylic group (δ_C 172.3, C8) in its $^1H-^{13}C$ HMBC 2D NMR spectrum (Figure S7 in the Supporting Information) suggest that this gastrodin moiety is in the form of esters, which have already been reported in this genus previously.[9−12]

Moreover, the $^1H-^{13}C$ HMBC spectrum (Figure S7 in the Supporting Information) of the cyclohexenic moiety (IV) showed long-range correlations for H2/C7 (δ_H 7.01/δ_C 167.1) and H6/C7 (δ_H 4.32/δ_C 167.1) indicating the attachment of a $-COOH$ group (C7) to C1 (δ_C 132.7); the correlations for H2/C8 (δ_H 7.01/δ_C 172.3) and H4/C8 (δ_H 3.03/δ_C 172.3) indicate the linkage of C3–C8 ($-COOH$) while the correlations for H3/C9 (δ_H 3.88/δ_C 173.9) and H4/C9 (δ_H 3.03/δ_C 173.9) suggest that C9 ($-COOH$) is linked to C4 (δ_C 37.8). Long-range correlations for H6 (δ_H 4.32) of the cyclohexenic moiety with two protonated carbons (C2′ at δ_C 116.4 and C6′ at δ_C 120.6) and a quarternary aromatic carbon (C1′ at δ_C 134.7) in fragment V (Figure S7 in the Supporting Information) suggest that these two fragments are linked together via a C6–C1′ bond. This was confirmed by

dx.doi.org/10.1021/jf204406u | J. Agric.Food Chem. 2012, 60, 129–135

Table 1. ^{1}H and ^{13}C NMR Data (from an 800 MHz Spectrometer) for Origanine A, B and C in CD_3CN

	origanine A		origanine B		origanine C	
no.	δ_H[a] (298 K)	δ_C	δ_H[a] (313 K)	δ_C	δ_H[a] (298 K)	δ_C
1		132.7		132.4		130.4
2	7.01 (br d, 3.3)	137.8	6.94 (br d, 3.3)	137.8	7.04 (d, 2.8)	139.4
3	3.88 (ddd, 10.3, 3.3, 1.8)	44.5	3.85 (ddd, 10.2, 3.3, 1.6)	44.4	3.41 (ddd, 10.1, 2.8, 1.9)	52.4
4	3.03 (dd, 10.3, 3.9)	37.8	3.08 (dd, 10.3, 4.0)	37.8	3.36 (dd, 12.5, 10.1)	39.7
5	3.26 (dd, 3.9, 2.2)	49.3	3.26 (dd, 4.0, 2.2)	49.4	3.29 (dd, 12.5, 5.7)	47.8
6	4.32 (dd, 2.2, 1.8)	42.6	4.38 (dd, 2.1, 1.6)	42.5	3.83 (dd, 5.7, 1.9)	44.5
7		167.1		167.1		166.3
8		172.3		172.3		172.4
9		173.9		173.9		172.6
10		173.5		172.4		171.5
1′		134.7		134.7		134.5
2′	6.66 (d, 2.2)	116.4	6.66 (d, 2.2)	116.5	6.62 (d, 2.2)	116.4
3′		146.2		146.2		145.5
4′		145.0		145.0		144.7
5′	6.69 (d, 8.2)	116.5	6.71 (d, 8.2)	116.6	6.65 (d, 8.2)	116.3
6′	6.41 (dd, 8.2, 2.2)	120.6	6.42 (dd, 8.2, 2.2)	120.7	6.45 (dd, 8.2, 2.2)	121.1
1″		131.3		131.5		131.2
2″	7.36 (d, 8.7)	131.2	7.36 (d, 8.7)	131.3	7.35 (d, 8.7)	131.3
3″	7.07 (d, 8.7)	117.8	7.08 (d, 8.7)	117.8	7.06 (d, 8.7)	117.8
4″		158.9		158.8		158.8
5″	7.07 (d, 8.7)	117.8	7.08 (d, 8.7)	117.8	7.06 (d, 8.7)	117.1
6″	7.36 (d, 8.7)	131.2	7.36 (d, 8.7)	131.3	7.35 (d, 8.7)	131.3
7″a	5.20 (d, 12.1)	68.1	5.20 (d, 12.1)	68.1	5.21 (d, 12.1)	67.7
7″b	5.12 (d, 12.1)	68.1	5.14 (d, 12.1)	68.1	5.14 (d, 12.1)	67.7
1‴	4.94 (d, 7.5)	101.8	4.94 (d, 7.2)	101.8	4.94 (d, 7.2)	101.8
2‴	3.39 (dd, 9.0, 7.5)	74.8	3.42 (*m*)	74.8	3.39 (*m*)	74.7
3‴	3.40 (dd, 9.0, 8.4)	77.7	3.42 (*m*)	77.8	3.40 (*m*)	77.9
4‴	3.32 (dd, 9.6, 8.4)	71.5	3.34 (dd, 9.0, 8.0)	71.5	3.33 (dd, 9.5, 8.0)	71.5
5‴	3.46 (ddd, 9.6, 6.0, 2.6)	77.8	3.46 (ddd, 9.6, 6.0, 2.6)	77.8	3.46 (ddd, 9.6, 5.9, 2.7)	77.7
6‴a	3.83 (dd, 12.0, 2.6)	62.9	3.84 (dd, 12.0, 2.6)	63.0	3.79 (dd, 12.0, 2.7)	62.8
6‴b	3.64 (dd, 12.0, 6.0)	62.9	3.67 (dd, 12.0, 6.0)	63.0	3.62 (dd, 12.0, 5.9)	62.8
1⁗				129.4		129.3
2⁗			6.76 (d, 2.2)	117.8	6.71 (d, 2.2)	117.8
3⁗				145.7		145.7
4⁗				144.9		144.9
5⁗			6.75 (d, 8.2)	116.5	6.70 (d, 8.2)	116.4
6⁗			6.64 (dd, 8.2, 2.2)	122.7	6.58 (dd, 8.2, 2.2)	122.7
7⁗a			3.07 (dd, 14.6, 4.3)	37.2	2.89 (dd, 14.4, 5.2)	37.5
7⁗b			2.96 (dd, 14.6, 8.2)	37.2	2.85 (dd, 14.6, 7.3)	37.5
8⁗			5.13 (dd, 8.2, 4.3)	74.5	4.79 (dd, 7.3, 5.2)	74.6
9⁗				170.8		170.9

[a]Multiplicity, *J*, Hz.

correlations (Figure S7 in the Supporting Information) for H2′/C6 (δ_H 6.66/δ_C 42.6) and H6′/C6 (δ_H 6.41/δ_C 42.6). Correlations between C10 (δ_C 173.5) with both H6 (δ_H 4.32) and H5 (δ_H 3.26) indicate the presence of the C5−C10 linkage. Therefore, the planar structure of this compound is determined as shown in Figure 3. To the best of our knowledge, such a cyclohexenetetracarboxylic acid skeleton has not been reported before.

There are four chiral carbons in such a skeleton, and the absolute configurations of them can normally be unambiguously determined with X-ray diffraction. However, several attempts to crystallize this compound all proved unsuccessful. Nevertheless, *J*-coupling constants for the protons in this skeleton also carry crucial information for the absolute configurations since *J*-coupling constants are dependent on the dihedral angles of the planes in which protons locate. Therefore, we calculated the *J*-coupling constants of all sixteen possible enantiomers for this compound (Table 2) with the density functional theory (DFT) calculations using the GIAO method at the B3LYP/6-311++G(d,p) level following full optimization for all the structures at the B3LYP/6-31G(d) level with Gaussian 03. By comparing the calculated values with experimental coupling constants, (3*S*,4*S*,5*S*,6*R*) stood out as the only reasonable possibility.

We further measured NOEs to confirm the spatial approximity of some protons in this molecule. The $^{1}H-^{1}H$ NOESY 2D NMR spectrum of this compound (Figure S5 in the Supporting Information) showed NOE correlations for H6′/H4, H6′/H5, H6′/H6, H2′/H4, H2′/H5 and H2′/H6 (Figure 4). This was consistent with the calculated interproton distances for these proton pairs (2.7, 4.1, 3.7, 4.2, 2.7 and 2.5 Å respectively) in the optimized (3*S*,4*S*,5*S*,6*R*)

dx.doi.org/10.1021/jf204406u | *J. Agric.Food Chem.* 2012, 60, 129−135

Table 2. Calculated *J*-Coupling Constants (Hz) for 16 Isomers of the Cyclohexene Skeleton in 1

no.	C3−C4−C5−C6	H2−H3	H3−H4	H4−H5	H5−H6	H2−H6	H3−H6
1	RSRR	6.6	1.6	5.3	8.5	1.1	1.2
2	SSSS	2.5	9.8	4.2	6.9	1.0	1.5
3	SSRS	2.6	9.5	10.6	8.2	2.7	4.6
4	SSRR	2.6	4.7	5.2	8.4	2.5	3.9
5	SRSS	2.4	4.8	2.4	7.9	2.1	3.5
6	SRSR	2.9	6.6	2.4	1.0	2.5	4.4
7	SRRR	2.7	6.3	4.7	7.4	1.9	3.3
8	SRRS	3.4	9.0	10.5	5.0	2.5	3.8
9	RSRS	7.1	4.9	12.2	6.7	1.3	1.8
10	RSSR	6.8	5.0	0	11.1	2.4	7.1
11	RRRR	4.3	1.0	4.2	4.6	2.3	1.1
12	RRSR	5.4	0.9	2.2	0.9	1.0	1.2
13	RSSS	6.2	6.6	3.8	7.9	1.5	1.2
14	RRSS	4.7	7.6	3.3	1.3	2.9	2.4
15	RRRS	4.8	7.3	11.0	6.0	0.9	1.0
16	SSSR	4.0	9.5	4.7	1.5	1.0	1.5
exptl		3.3	10.4	3.9	2.1	<1.0	1.8

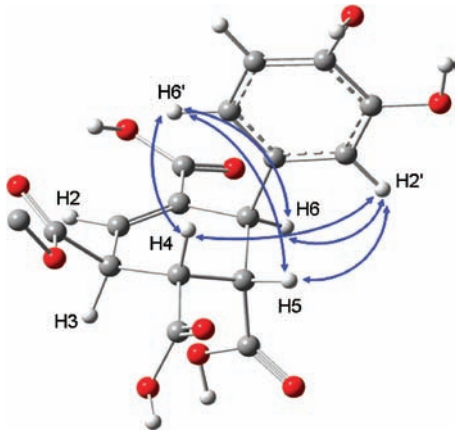

Figure 4. Key NOEs observed in the novel skeleton of origanine A (**1**).

structure. Therefore, the structure was determined to have a 4-(*β*-D-glucopyranosyloxy)benzyl alcohol moiety attached to C8 of (3*S*,4*S*,5*S*,6*R*)-6-(3,4-dihydroxybenzyl)cyclohexene-1,3,4,5-tetracarboxylic acids.

Origanine B (**2**) was initially detected in the LC−MS analysis (in the negative ion mode) with a *quasimolecular* ion at *m*/*z* 813.1896 (Figure 2B), and thus $C_{38}H_{38}O_{20}$ was suggested as its molecular formula (calcd *m*/*z* 813.1884 for $C_{38}H_{37}O_{20}$, with an error of 1.2 mDa). The number of carbons in it was confirmed with its $^{1}H-^{13}C$ HMBC 2D NMR spectrum (Figure S12 in the Supporting Information).

The planar structure of **2** was determined in the same fashion as in the case of **1** using 2D NMR spectra (Figures S9−S12 in the Supporting Information); **2** was found to be a derivative of **1** having similar structural fragments I−V. However, this compound had two more ABX coupling systems in its ^{1}H NMR spectrum (Figure S8 in the Supporting Information) than **1**, which was easily observed in its $^{1}H-^{1}H$ COSY (Figure S9 in the Supporting Information) and TOCSY 2D NMR spectra (Figure S10 in the Supporting Information). One ABX system had three protons at δ_H 5.13 (1H, dd, *J* = 8.2, 4.3 Hz, H8′′′′), 3.07 (1H, dd, *J* = 14.6, 4.3 Hz, H7′′′′a) and 2.96 (1H, dd, *J* = 14.6, 8.2 Hz, H7′′′′b) in the aliphatic region, being consistent with a $-CH_2CHO-$ moiety (fragment VI). The other ABX system with three protons at δ_H 6.76 (1H, d, *J* = 2.2 Hz, H2′′′′), 6.75 (1H, d, *J* = 8.2 Hz, H5′′′′) and 6.64 (1H, dd, *J* = 8.2, 2.2 Hz, H6′′′′) in the aromatic region was readily assigned to a 3,4-dihydroxyphenyl moiety (fragment VII). These two fragments had typical spectral features found for 3-(3,4-dihydroxyphenyl)-lactic acid (i.e., danshensu) residue. This was supported with a fragment loss of 198 Da in its mass spectrum (Figure 2 B, from *m*/*z* 813.1896 to *m*/*z* 615.1365). The $^{1}H-^{13}C$ HMBC 2D NMR spectrum (Figure S12 in the Supporting Information) of this compound further showed that the fragment V was attached to C10 (−COO−) of cyclohexene skeleton via an ester linkage with the observation of long-range correlation for H8′′′′/C10 (δ_H 5.11/δ_C 172.4) (Figure S12 in the Supporting Information). Since this compound had *J*-coupling constants for the skeleton protons similar to what **1** had, the absolute configuration for the skeleton carbons ought to be the same as for **1**.

The third new metabolite, origanine C (**3**), was detected as an isomer of **2** with a similar *quasimolecular* ion at *m*/*z* 813.1864 (Figure 3C) and thus the same molecular formula (calcd *m*/*z* 813.1884 for $C_{38}H_{37}O_{20}$, with an error of 2.0 mDa); the number of carbons in **3** was also confirmable with $^{1}H-^{13}C$ HMBC 2D NMR data (Figure S1 in the Supporting Information7). This compound showed some fragment ions at *m*/*z* 769.1966 and 571.1426, corresponding to the loss of −COOH and 3-(3,4-dihydroxyphenyl)lactic acid moieties (danshensu).

However, two major differences were observable for this compound compared with **2** in terms of structural features. $^{1}H-^{13}C$ HMBC 2D NMR spectrum of this compound (Figure S17 in the Supporting Information) showed that the fragment V and a COOH group were linked to C4 and C6 of the cyclohexene skeleton, respectively, while the 4-(*β*-D-glucopyranosyloxy)benzyl alcohol moiety was attached to the carboxylic group on C1 (see long-range correlations in Figure 3). The *J*-coupling constants for cyclohexenic skeleton protons in **3** were also clearly different from those in both **1** and **2**. The DFT results for *J*-coupling constants (Table 3) indicated that, among all possibilities, only (3*S*,4*R*,5*S*,6*S*)-cyclohexene was in good agreement with the experimental data for all these skeleton chiral carbons of this compound. Therefore, its absolute configuration for the skeleton was determined as (3*S*,4*R*,5*S*,6*S*)-4-(3,4-dihydroxybenzyl)cyclohexene-1,3,5,6-tetracarboxylic acid (Figure 3). The observation of NOEs for H2′/H3, H2′/H5, H6′/H3 and H6′/H5 (Figure S18 in the Supporting Information) was consistent with the calculated interproton distances for these proton pairs (4.3, 4.6, 2.5 and 2.4 Å respectively) in the optimized (3*S*,4*R*,5*S*,6*S*) structure, further supporting such configurations for the skeleton carbons.

An exhaustive literature search indicates that neither these three polyphenolic compounds nor the skeleton of cyclohexenetetracarboxylic acids has been reported previously. The findings in this work indicate that new metabolites, especially metabolites with new skeletons, remain to be further discovered. The results have also demonstrated that the LC-DAD-SPE-NMR/MS methods are powerful in discovering some potentially interesting new compounds, especially those with novel skeletons, even in the plants which have been considered as well-studied.

It is natural to be curious about the potential bioactivities of these new compounds. Although we do not have enough

dx.doi.org/10.1021/jf204406u | *J. Agric.Food Chem.* 2012, 60, 129−135

Table 3. Calculated *J*-Coupling Constants (Hz) for 16 Isomers of the Cyclohexene Skeleton in 3

no.	C3−C4−C5−C6	H2−H3	H3−H4	H4−H5	H5−H6	H2−H6	H3−H6
1	RSRR	4.9	0.8	2.1	6.4	3.1	3.5
2	SSSS	2.6	7.0	5.1	8.6	2.7	4.1
3	SSRS	3.0	6.7	3.0	1.3	1.9	2.7
4	SSRR	2.8	6.7	2.9	6.3	5.5	4.2
5	SSSR	2.6	6.7	5.2	9.1	2.4	4.0
6	SRSR	3.3	9.1	11.0	9.4	2.9	4.9
7	SRRR	3.1	9.7	4.5	6.5	0	4.5
8	SRRS	4.5	9.9	4.5	1.7	1.1	1.6
9	RSRS	4.6	0.8	1.8	1.3	1.5	1.2
10	RSSR	6.3	7.2	5.3	9.6	2.6	2.9
11	RRRR	6.0	6.4	2.9	6.2	3.0	2.9
12	RRSR	5.5	6.2	10.7	9.1	2.9	2.7
13	RSSS	6.6	0.7	6.9	9.7	2.8	1.7
14	RRSS	5.1	6.5	11.0	5.7	1.4	0.8
15	RRRS	5.4	7.0	3.0	1.2	1.3	0.9
16	SRSS	4.0	8.7	11.3	5.4	1.1	2.3
exptl		2.8	10.1	12.5	5.7	<1	1.9

materials for the bioactivity investigation at the moment, some predictions are possible with plenty of information available for the structural fragments found in these new compounds. Structrural features of these new compounds imply that they may have multiple bioactivities since 4-(β-D-glucopyranosyloxy)benzyl alcohol (gastrodin), 3,4-dihydroxyphenyl and 3-(3,4-dihydroxyphenyl)lactic acid (danshensu) residues are well-known for their antioxidant activies. In fact, danshensu is a major bioactive component of *Salvia miltiorrhiza*[25] used for treating cardiovascular conditions whereas gastrodin has long been used for treating epilepsy, stroke and dementia with its neuroprotective bioactivities and ability to cross the blood−brain barrier.[26] Synergistic effects appear to be a reasonable proposition with these residues linked together. It is apparent that the development of efficient methods for their synthesis will be vital for further exploration of their bioactivities and that their biosynthesis also need further investigating. Nevertheless, the findings in this study will inevitably promote a new wave of research activities in discovering novel compounds having new skeletons in natural sources with these hyphenated methods. Such activities will be important not only for drug discoveries from the plant sources but also for further understanding of the plant secondary metabolisms.

■ ASSOCIATED CONTENT

Supporting Information

Ultraviolet−visible spectra, 1D and 2D NMR spectra of **1**, **2** and **3**. This material is available free of charge via the Internet at http://pubs.acs.org.

■ AUTHOR INFORMATION

Corresponding Author

*Tel: +86-(0)27-87198430. E-mail: huiru.tang@wipm.ac.cn.

Author Contributions

§These authors contributed equally to this work.

Funding

We acknowledge financial support from the National Basic Research Program of China (2010CB912501), the National Natural Science Foundation of China (20825520, 20921004, 211-75149), Ministry of Agriculture of China (2009ZX08012-023B) and Chinese Academy of Sciences (KJCX2-YW-W13 and KSCX1-YW-W02).

■ REFERENCES

(1) Kintzios, S. E. *Oregano: The Genera Origanum and Lippia (Medicinal and Aromatic Plants-Industrial Profiles)*; CRC Press: New York, 2002.

(2) Kintzios, S. E. *Sage: The Genus Salvia (Medicinal and aromatic plants-Industrial profiles)*; CRC Press: London, UK, 2000.

(3) Hiltunen, R. *Basil: The Genus Ocimum (Medicinal and aromatic plants-Industrial profiles)*; CRC Press: London, UK, 1999.

(4) Lawrence, B. M. *Mint: The Genus Mentha (Medicinal and aromatic plants-Industrial profiles)*; CRC Press: London, UK, 2006.

(5) Chen, C.; Tang, H. R.; Sutcliffe, L. H.; Belton, P. S. Green tea polyphenols react with 1,1-diphenyl-2-picrylhydrazyl free radicals in the bilayer of liposomes: direct evidence from electron spin resonance studies. *J. Agric. Food Chem.* **2000**, *48*, 5710−5714.

(6) Lu, Z. B.; Nie, G. J.; Belton, P. S.; Tang, H. R.; Zhao, B. L. Structure-activity relationship analysis of antioxidant ability and neuroprotective effect of gallic acid derivatives. *Neurochem. Int.* **2006**, *48*, 263−274.

(7) Lawrence, B. M. *The Antimicrobial/Biological Activity of Essential Oils*; Allured Publishing Corporation: Carol Stream, IL, 2005.

(8) Koukoulitsa, C.; Karioti, A.; Bergonzi, M. C.; Pescitelli, G.; Di Bari, L.; Skaltsa, H. Polar constituents from the aerial parts of *Origanum vulgare* L. *ssp hirtum* growing wild in Greece. *J. Agric. Food Chem.* **2006**, *54*, 5388−5392.

(9) Takeda, Y.; Tomonari, M.; Arimoto, S.; Masuda, T.; Otsuka, H.; Matsunami, K.; Honda, G.; Ito, M.; Takaishi, Y.; Kiuchi, F.; Khodzhimatov, O. K.; Ashurmetov, O. A. A new phenolic glucoside from an Uzbek medicinal plant, *Origanum tyttanthum*. *J. Nat. Med.* **2008**, *62*, 71−74.

(10) Lin, Y. L.; Wang, C. N.; Shiao, Y. J.; Liu, T. Y.; Wang, W. Y. Benzolignanoid and polyphenols from *Origanum vulgare*. *J. Chin. Chem. Soc.* **2003**, *50*, 1079−1083.

(11) Liang, C. H.; Chou, T. H.; Ding, H. Y. Inhibition of melanogensis by a novel origanoside from *Origanum vulgare*. *J. Dermatol. Sci.* **2010**, *57*, 170−177.

(12) Nakatani, N.; Kikuzaki, H. A new antioxidative glucoside isolated from oregano (*Origanum vulgare* L.). *Agric. Biol. Chem.* **1987**, *51*, 2727−2732.

(13) Skaltsa, H.; Chatzopoulou, A.; Karioti, A.; Gousiadou, C.; Vivancos, V. L.; Kyriazopoulos, P.; Golegou, S. Depsides and other polar constituents from *Origanum dictamnus* L. and their *in vitro* antimicrobial activity in clinical strains. *J. Agric. Food Chem.* **2010**, *58*, 6064−6068.

(14) Xiao, C. N.; Dai, H.; Liu, H. B.; Wang, Y. L.; Tang, H. R. Revealing the metabonomic variation of rosemary extracts using ^{1}H NMR spectroscopy and multivariate data analysis. *J. Agric. Food Chem.* **2008**, *56*, 10142−10153.

(15) Dai, H.; Xiao, C. N.; Liu, H. B.; Tang, H. R. Combined NMR and LC-MS analysis reveals the metabonomic changes in *Salvia miltiorrhiza* Bunge induced by water depletion. *J. Proteome Res.* **2010**, *9*, 1460−1475.

(16) Dai, H.; Xiao, C. N.; Liu, H. B.; Hao, F. H.; Tang, H. R. Combined NMR and LC-DAD-MS analysis reveals comprehensive metabonomic variations for three phenotypic cultivars of *Salvia miltiorrhiza* Bunge. *J. Proteome Res.* **2010**, *9*, 1565−1578.

(17) Tang, H. R.; Xiao, C. N.; Wang, Y. L. Important roles of the hyphenated HPLC-DAD-MS-SPE-NMR technique in metabonomics. *Magn. Reson. Chem.* **2009**, *47*, S157−S162.

(18) Exarchou, V.; Godejohann, M.; van Beek, T. A.; Gerothanassis, I. P.; Vervoort, J. LC-UV-solid-phase extraction-NMR-MS combined with a cryogenic flow probe and its application to the identification of compounds present in Greek oregano. *Anal. Chem.* **2003**, *75*, 6288−6294.

(19) Holmes, E.; Tang, H. R.; Wang, Y. L.; Seger, C. The assessment of plant metabolite profiles by NMR based methodologies. *Planta Med.* **2006**, *72*, 771−785.

(20) Rasmussen, B.; Cloarec, O.; Tang, H. R.; Staerk, D.; Jaroszewski, J. W. Multivariate analysis of integrated and full-resolution ^{1}H-NMR spectral data from complex pharmaceutical preparations: St. John's Wort. *Planta Med.* **2006**, *72*, 556−563.
(21) Liu, C. X.; Hao, F. H.; Hu, J.; Zhang, W. L.; Wan, L. L.; Zhu, L. L.; Tang, H. R.; He, G. C. Revealing different systems responses to brown planthopper infestation for pest susceptible and resistant rice plants with the combined metabonomic and gene-expression analysis. *J. Proteome Res.* **2010**, *9*, 6774−6785.
(22) Chen, F. F.; Zhang, J. T.; Song, X. S.; Yang, J.; Li, H. P.; Tang, H. R.; Liao, Y. C. Combined metabonomic and quantitative real-time PCR analyses reveal systems metabolic changes of *Fusarium graminearum* induced by Tri5 gene deletion. *J. Proteome Res.* **2011**, *10*, 2273−2285.
(23) Zhang, J. T.; Zhang, Y.; Du, Y. Y.; Chen, S. Y.; Tang, H. R. Dynamic metabonomic responses of tobacco (*Nicotiana tabacum*) plants to salt stress. *J. Proteome Res.* **2011**, *10*, 1904−1914.
(24) Pretsch, E.; Bühlmann, P.; Affolter, C. *Structure Determination of Organic Compounds: Tables of Spectral Data*; Springer: Berlin, Gemany, 2000; p 168.
(25) Jiang, R. W.; Lau, K. M.; Hon, P. M.; Mak, T. C.; Woo, K. S.; Fung, K. P. Chemistry and biological activities of caffeic acid derivatives from *Salvia miltiorrhiza*. *Curr. Med. Chem.* **2005**, *12*, 237−246.
(26) Lin, L. C.; Chen, Y. F.; Tsai, T. R.; Tsai, T. H. Analysis of brain distribution and biliary excretion of a nutrient supplement, gastrodin, in rat. *Anal. Chim. Acta* **2007**, *590*, 173−179.